

See discussions, stats, and author profiles for this publication at: <https://www.researchgate.net/publication/26765943>

# Fluorescence Lifetime Multiplexing with Nanocrystals and Organic Labels

ARTICLE in ANALYTICAL CHEMISTRY · SEPTEMBER 2009

Impact Factor: 5.64 · DOI: 10.1021/ac900934a · Source: PubMed

CITATIONS

25

READS

45

6 AUTHORS, INCLUDING:



**Peter Kapusta**

Academy of Sciences of the Czech Republic

56 PUBLICATIONS 601 CITATIONS

SEE PROFILE



**Thomas Nann**

Victoria University of Wellington

126 PUBLICATIONS 4,680 CITATIONS

SEE PROFILE



**Ute Resch-Genger**

Bundesanstalt für Materialforschung und -...

179 PUBLICATIONS 5,115 CITATIONS

SEE PROFILE

# Fluorescence Lifetime Multiplexing with Nanocrystals and Organic Labels

Markus Grabolle,<sup>†</sup> Peter Kapusta,<sup>‡</sup> Thomas Nann,<sup>§</sup> Xu Shu,<sup>§</sup> Jan Ziegler,<sup>§</sup> and Ute Resch-Genger<sup>\*†</sup>

BAM Federal Institute for Materials Research and Testing, Richard-Willstaetter-Strasse 11, 12489 Berlin, Germany, PicoQuant GmbH, Rudower Chaussee 29, 12489 Berlin, Germany, and School of Chemistry, University of East Anglia (UEA), Norwich NR4 7TJ, U.K.

The potential of semiconducting nanocrystals or so-called quantum dots (QDs) for lifetime multiplexing has not been investigated yet, despite the increasing use of QDs in (bio)analytical detection, biosensing, and fluorescence imaging and the obvious need for simple and cost-effective tools and strategies for the simultaneous detection of multiple analytes or events. This is most likely related to their multiexponential decay behavior as for multiplex chromophores, typically monoexponential decay kinetics are requested. The fluorescence decay kinetics of various mixtures of a long-lived, multiexponentially decaying CdSe QD and a short-lived organic dye were analyzed, and a model was developed for the quantification of these labels from the measured complex decay kinetics as a first proof-of-concept for the huge potential of these labels for lifetime multiplexing. In a second step, we evaluated the potential of mixtures of two types of QDs, varying in constituent material to realize distinguishable, yet multiexponential decay kinetics and similar absorption and emission spectra. Strategies for lifetime multiplexing with nanocrystalline labels were derived on the basis of these measurements.

Current security and health concerns require robust, cost-effective, and efficient tools and strategies for the simultaneous analysis and detection of multiple analytes or events in parallel. The ability to screen for and quantify multiple targets in a single assay or measurement, termed multiplexing, allows one to reduce the amount of reagents, consumables, and sample required, decrease sampling errors, and ease the inclusion of internal controls. The most striking examples for multiplexed assays are planar microarrays<sup>1–8</sup> and encoded bead or microcarrier array platforms that increase assay performance in the liquid phase

(suspension array) and can be combined, e.g., with a flow cytometric system.<sup>9–18</sup>

The vast majority of multiplexing applications combine local resolution of different targets with detection methods that enable preferably the simultaneous measurement of different analyte-specific parameters. The local resolution is provided by either positioning selective capture reagents on a planar substrate such as a microarray or by separation techniques like capillary gel electrophoresis, high-performance liquid chromatography (HPLC), or flow cytometry. This increases the number of measurable species and reduces the requirements on the multiplexing capability of the read-out technique. Detection methods suitable for multiplexed analysis include fluorescence techniques,<sup>9–18</sup> Raman spectroscopy,<sup>19,20</sup> electrochemistry,<sup>21</sup> and laser ablation inductively coupled plasma mass spectrometry (ICPMS).<sup>22–24</sup> At present, the majority of multiplexing applications involves the measurement of photoluminescence.<sup>9–18</sup> Photoluminescence techniques are not only easy to use, are comparatively inexpensive, and provide a

- (7) Marshall, A.; Hodgson, J. *Nat. Biotechnol.* **1998**, *16*, 27–31.
- (8) Lander, E. S. *Nat. Genetics (Suppl.)* **1999**, *21*, 3–4.
- (9) Nolan, J. P.; Mandy, F. *Cytometry, Part A* **2006**, *69A*, 318–325.
- (10) Fulton, R. J.; McDade, R. L.; Smith, P. L.; Kienker, L. J.; Kettman, J. R. *Clin. Chem.* **1997**, *43*, 1749–1756.
- (11) Beske, O.; Guo, J. J.; Li, J. R.; Bassoni, D.; Bland, K.; Marciniak, H.; Zarowitz, M.; Temov, V.; Ravkin, I.; Goldbard, S. *J. Biomol. Screening* **2004**, *9*, 173–185.
- (12) Uguzzoli, L. A. *Clin. Chem.* **2004**, *50*, 1963–1965.
- (13) Eastman, P. S.; Ruan, W.; Doctolero, M.; Nuttall, R.; de Freo, G.; Park, J. S.; Chu, J. S. F.; Cooke, P.; Gray, J. W.; Li, S.; Chen, F. F. *Nano Lett.* **2006**, *6*, 1059–1064.
- (14) Riegger, L.; Grumann, M.; Nann, T.; Riegler, J.; Ehler, O.; Bessler, W.; Mittenbuehler, K.; Urban, G.; Pastewka, L.; Brenner, T.; Zengerle, R.; Ducre, J. *Sens. Actuators, A: Phys.* **2006**, *126*, 455–462.
- (15) Shepard, J. R. E. *Anal. Chem.* **2006**, *78*, 3589–3597.
- (16) Ferguson, J. A.; Steemers, F. J.; Walt, D. R. *Anal. Chem.* **2000**, *72*, 5618–5624.
- (17) Evans, M.; Sewter, C.; Hill, E. *Assay Drug Dev. Technol.* **2003**, *1*, 199–207.
- (18) Zhi, Z.; Morita, Y.; Hasan, Q.; Tamiya, E. *Anal. Chem.* **2003**, *75*, 4125–4131.
- (19) Docherty, F. T.; Monaghan, P. B.; Keir, R.; Graham, D.; Smith, W. E.; Cooper, J. M. *Chem. Commun.* **2004**, 118–119.
- (20) Stokes, R. J.; Macaskill, A.; Lundahl, P. J.; Smith, W. E.; Faulds, K.; Graham, D. *Small* **2007**, *3*, 1593–1601.
- (21) Liu, G.; Wang, J.; Kim, J.; Greg, M. R. J.; Collins, E. *Anal. Chem.* **2004**, *76*, 7126–7130.
- (22) Hu, S.; Zhang, S.; Hu, Z.; Xing, Z.; Zhang, X. *Anal. Chem.* **2007**, *79*, 923–929.
- (23) Ornatsky, O.; Baranov, V.; Bandura, D. R.; Tanner, S. D.; Dick, J. J. *Immunol. Methods* **2006**, *308*, 68–76.
- (24) Roos, P. H.; Venkatachalam, A.; Manz, A.; Waentig, L.; Koehler, C. U.; Jakubowski, N. *Anal. Bioanal. Chem.* **2008**, *392*, 1135–1147.

\* To whom correspondence should be addressed. E-mail: ute.resch@bam.de. Phone: ++49(0)30-8104-1134. Fax: ++49(0)30-8104-1159.

<sup>†</sup> BAM Federal Institute for Materials Research and Testing.

<sup>‡</sup> PicoQuant GmbH.

<sup>§</sup> University of East Anglia (UEA).

- (1) Nagl, S.; Schaeferling, M.; Wolfbeis, O. S. *Microchim. Acta* **2005**, *151*, 1–21.
- (2) Bally, M.; Halter, M.; Voros, J.; Grandin, H. M. *Surf. Interface Anal.* **2006**, *38*, 1442–1458.
- (3) Schaeferling, M.; Nagl, S. *Anal. Bioanal. Chem.* **2006**, *385*, 500–517.
- (4) Tezak, Z.; Ranamukhaarachchi, D.; Russek-Cohen, E.; Gutman, S. I. *Hum. Genomics* **2006**, *2*, 236–243.
- (5) Hoheisel, J. D. *Nat. Rev. Genetics* **2006**, *7*, 200–210.
- (6) Shi, L.; Tong, W.; Goodsaid, F.; Frueh, F. W.; Fang, H.; Han, T.; Fuscoe, J. C.; Casciano, D. A. *Expert Rev. Mol. Diagn.* **2004**, *4*, 761–777.

sensitivity down to the single molecule level, yet they offer access to several analyte-specific parameters such as emission spectra, fluorescence intensity (quantum yield), fluorescence lifetime, and emission anisotropy. Spectral multiplexing (multicolor signaling) is the most common multiplexing method. Here, different fluorophores, excited at a single or different excitation wavelengths, are discriminated by their emission wavelength. Spectral multiplexing with organic dyes is mostly limited to the discrimination of two species due to their comparatively broad emission bands of slightly structured shape and the narrow wavelength region of optimal excitation of each dye. The number of distinguishable labels can be increased to, e.g., three or four either using different measurements conditions and pattern recognition,<sup>25</sup> multiwavelength excitation,<sup>26,27</sup> or donor–acceptor dye combinations to increase the spectral separation of absorption and emission via fluorescence resonance energy transfer (FRET).<sup>28–30</sup> Lanthanide labels are better suited for color multiplexing because they show very narrow emission bands and large Stokes shift. However, with the exception of upconverting materials,<sup>31</sup> they require unfavorable short-wavelength excitation below ~400 nm in the absorption region of the ligand.<sup>32,33</sup> The most promising labels for this type of detection are nanocrystalline chromophores such as quantum dots (QDs) with their size-tunable absorption and emission properties.<sup>34–37</sup> The extremely broad absorption spectra of QDs enable efficient multilabel excitation and their narrow and symmetric emission bands simplify color discrimination and reduce spectral overlap. All these fluorophores can be incorporated into nanometer- or micrometer-sized organic or inorganic particles for the generation of color- and intensity-encoded labels or supports for multiplexed assays.<sup>31,37–42</sup>

Alternatively, fluorescence multiplexing can be performed in the time domain, utilizing the fluorophore-specific fluorescence lifetime to discriminate between different chromophores, prefer-

ably measured at a single excitation and a single emission wavelength.<sup>43–49</sup> This approach is less sensitive to fluctuations in the excitation light intensity and to crosstalk (overlapping emission spectra) but requires sufficiently different lifetimes of the labels.<sup>50</sup> This limits the number of distinguishable organic fluorophores, the lifetimes of which, with very few exceptions, covering only the region of 1–6 ns.<sup>51</sup> Moreover, typically monoexponential decay kinetics have been requested for this application up to now. Lifetime multiplexing has been exclusively realized with organic chromophores, typically in combination with separation techniques like HPLC, capillary electrophoresis, or flow cytometry despite its obvious potential and the progress in laser and detector technology, rendering time-resolved fluorometry more and more affordable.<sup>43,44,51–56</sup> Lanthanide chelates have been used in homogeneous time-resolved fluorometric immunoassays (TR-FIA) using time-gated detection and time windows (DELTA technology).<sup>57,58</sup> To the best of our knowledge, up until now, there are no reports on the use of QDs for lifetime multiplexing apart from one single exception.<sup>59</sup> The attractive long lifetime of QDs in the order of 10–100 ns has been exploited for time-gated biological imaging<sup>60</sup> or for time-resolved fluorescence resonance energy transfer (TR-FRET) assays.<sup>59,61,62</sup> This is most likely related to the fact that in general QDs show multiexponential

- (25) Kobayashi, H.; Koyama, Y.; Barrett, T.; Hama, Y.; Regino, C. A. S.; Shin, I. S.; Jang, B. S.; Le, N.; Paik, C. H.; Choyke, P. L.; Urano, Y. *ACS Nano* **2007**, *1*, 258–264.
- (26) Lewis, E. K.; Haaland, W. C.; Nguyen, F.; Heller, D. A.; Allen, M. J.; MacGregor, R. R.; Berger, C. S.; Willingham, B.; Burns, L. A.; Scott, G. B. I.; Kittrell, C.; Johnson, B. R.; Curl, R. F.; Metzker, M. L. *Proc. Natl. Acad. Sci. U.S.A.* **2005**, *102*, 5346–5351.
- (27) De Rosa, S. C.; Brenchley, J. M.; Roederer, M. *Nat. Med.* **2003**, *9*, 112–117.
- (28) Ju, J. Y.; Ruan, C. C.; Fuller, C. W.; Glazer, A. N.; Mathies, R. A. *Proc. Natl. Acad. Sci. U.S.A.* **1995**, *92*, 4347–4351.
- (29) Sapsford, K. E.; Berti, L.; Medintz, I. L. *Angew. Chem., Int. Ed.* **2006**, *45*, 4562–4588.
- (30) Resch-Genger, U.; Grabolle, M.; Cavaliere-Jaricot, S.; Nitschke, R.; Nann, T. *Nat. Methods* **2008**, *5*, 763–775.
- (31) Ehlert, O.; Thomann, R.; Darbandi, M.; Nann, T. *ACS Nano* **2008**, *2*, 120–124.
- (32) Yuan, J. L.; Wang, G. L. *TrAC, Trends Anal. Chem.* **2006**, *25*, 490–500.
- (33) Hemmila, I.; Laitala, V. J. *Fluoresc.* **2005**, *15*, 529–542.
- (34) Goldman, E. R.; Clapp, A. R.; Anderson, G. P.; Uyeda, H. T.; Mauro, J. M.; Medintz, I. L.; Mattoussi, H. *Anal. Chem.* **2004**, *76*, 684–688.
- (35) Michalet, X.; Pinaud, F. F.; Bentolila, L. A.; Tsay, J. M.; Doose, S.; Li, J. J.; Sundaresan, G.; Wu, A. M.; Gambhir, S. S.; Weiss, S. *Science* **2005**, *307*, 538–544.
- (36) Xing, Y.; Chaudry, Q.; Shen, C.; Kong, K. Y.; Zhou, H. E.; Chung, L. W.; Petros, J. A.; O'Regan, R. M.; Yezhelyev, M. V.; Simons, J. W.; Wang, M. D.; Nie, S. *Nat. Protoc.* **2007**, *2*, 1152–1165.
- (37) Sharma, P.; Brown, S.; Walter, G.; Santra, S.; Moudgil, B. *Adv. Colloid Interface Sci.* **2006**, *123–126*, 471–485.
- (38) Battersby, B. J.; Trau, M. *Aust. J. Chem.* **2007**, *60*, 343–353.
- (39) Seydack, M. *Biosens. Bioelectron.* **2005**, *20*, 2454–2469.
- (40) Yan, J. L.; Estevez, M. C.; Smith, J. E.; Wang, K. M.; He, X. X.; Wang, L.; Tan, W. H. *Nano Today* **2007**, *2*, 44–50.
- (41) Sukhanova, A.; Susha, A. S.; Bek, A.; Mayilo, S.; Rogach, A. L.; Feldmann, J.; Oleinikov, V.; Revel, B.; Donvito, B.; Cohen, J. H. M.; Nabiev, I. *Nano Lett.* **2007**, *7*, 2322–2327.
- (42) Gaponik, N.; Radtchenko, I. L.; Sukhorukov, G. B.; Weller, H.; Rogach, A. L. *Adv. Mater.* **2002**, *14*, 879–882.
- (43) Snalley, M. B.; McGown, L. B. *Anal. Chem.* **1995**, *67*, 1371–1376.
- (44) Keij, J. F.; Steinkamp, J. A. *Cytometry* **1998**, *33*, 318–323.
- (45) Sauer, M.; Schulz, A.; Seeger, S.; Wolfrum, J.; Ardenjacob, J.; Deltau, G.; Drexhage, K. H. *Ber. Bunsen-Ges.:Phys. Chem. Chem. Phys.* **1993**, *97*, 1734–1737.
- (46) Lassiter, S. J.; Stryjewski, W. J.; Wang, Y.; Soper, S. A. *Spectroscopy* **2002**, *17*, 14–+.
- (47) Carlsson, K.; Liljeborg, A. J. *Microsc.* **1997**, *185*, 37–46.
- (48) Ma, G.; Fortier, S.; Jean-Jacques, M.; Mincin, N.; Leblond, F.; Ichalalene, Z.; Benyamin-Seeyar, A.; Khayat, M. *Multimodal Biomed. Imaging III* **2008**, 6850, 85003–85003.
- (49) Bright, F. V.; McGown, L. B. *Anal. Chem.* **1985**, *57*, 55–59.
- (50) Nunnally, B. K.; He, H.; Li, L. C.; Tucker, S. A.; McGown, L. B. *Anal. Chem.* **1997**, *69*, 2392–2397.
- (51) Mihindukulasuriya, S. H.; Morcone, T. K.; McGown, L. B. *Electrophoresis* **2003**, *24*, 20–25.
- (52) Lieberwirth, U.; Arden-Jacob, J.; Drexhage, K. H.; Hertel, D. P.; Muller, R.; Neumann, M.; Schulz, A.; Siebert, S.; Sagner, G.; Klingel, S.; Sauer, M.; Wolfrum, J. *Anal. Chem.* **1998**, *70*, 4771–4779.
- (53) Sauer, M.; Arden-Jacob, J.; Drexhage, K. H.; Marx, N. J.; Karger, A. E.; Lieberwirth, U.; Muller, M.; Neumann, M.; Nord, S.; Paulus, A.; Schulz, A.; Seeger, S.; Zander, C.; Wolfrum, J. *Biomed. Chromatogr.* **1997**, *11*, 81–82.
- (54) Zhu, L.; Stryjewski, W. J.; Soper, S. A. *Anal. Biochem.* **2004**, *330*, 206–218.
- (55) Zhu, L.; Stryjewski, W.; Lassiter, S.; Soper, S. A. *Anal. Chem.* **2003**, *75*, 2280–2291.
- (56) Snyder, T. M.; McGown, L. B. *Appl. Spectrosc.* **2005**, *59*, 335–339.
- (57) Hemmila, I.; Webb, S. *Drug Discovery Today* **1997**, *2*, 373–381.
- (58) Watanabe, K.; Arakawa, H.; Maeda, M. *Luminescence* **2002**, *17*, 123–129.
- (59) Grabolle, M.; Pfeifer, L.; Stein, C.; Resch-Genger, U. *Luminescence* **2008**, *23*, 226–227.
- (60) Dahan, M.; Laurence, F.; Pinaud, F.; Chemla, D. S.; Alivisatos, A. P.; Sauer, M.; Weiss, S. *Opt. Lett.* **2001**, *26*, 825–827.
- (61) Medintz, I. L.; Konner, J. H.; Clapp, A. R.; Stanish, I.; Twigg, M. E.; Mattoussi, H.; Mauro, J. M.; Deschamps, J. R. *Proc. Natl. Acad. Sci. U.S.A.* **2004**, *101*, 9612–9617.
- (62) Charbonniere, L. J.; Hildebrandt, N.; Ziessel, R. F.; Loehmannsroeben, H. G. *J. Am. Chem. Soc.* **2006**, *128*, 12800–12809.

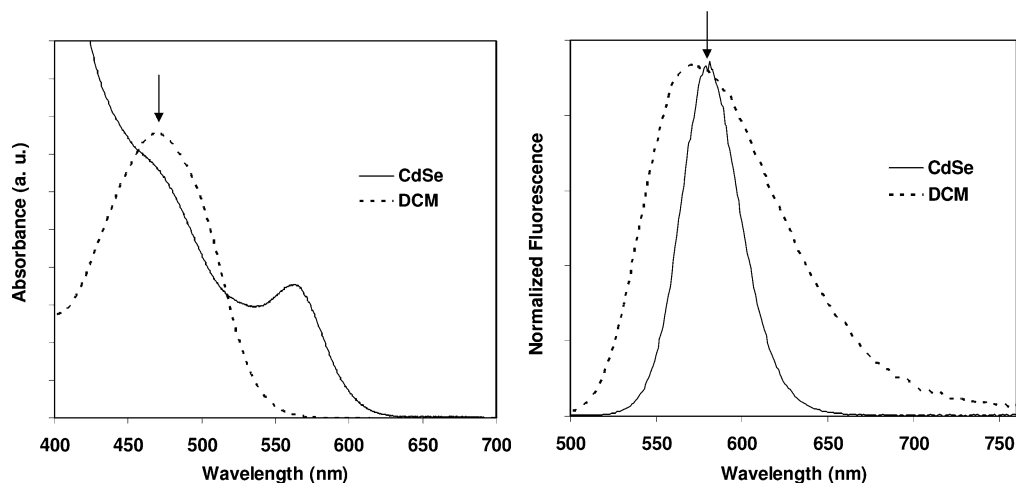


**Figure 1.** Absorption (left) and fluorescence (right) spectra of CdSe quantum dots (solid lines) and DCM (dashed lines) used for the CdSe–DCM mixtures. The arrows indicate the chosen excitation (466 nm) and detection (578 nm) wavelength.

decay kinetics, that can be observed even at the single molecule level, the origin of which is still under investigation.<sup>63,64</sup>

This encouraged us to evaluate the potential of QDs for lifetime multiplexing and searching for simple data evaluation procedures to take their multiexponential decay kinetics into account. The suitability of combinations of QDs and organic dyes as well as QDs of different constituent material was investigated as a first proof-of-concept for the potential of these labels for lifetime multiplexing. In a first step, the fluorescence decay kinetics of various mixtures of CdSe QDs and the organic dye DCM were analyzed and a model for the quantification of these fluorophores from the measured complex decay kinetics was developed. In a second step, we evaluated the potential of mixtures of two different types of QDs of complex decay kinetics, here CdSe and InP. It has to be emphasized that the “one-pot” approach presented here requires no further separation technique as is the case for most of the multiplexing strategies employed.

## INSTRUMENTATION AND MATERIALS

**Spectroscopy.** The absorption spectra were recorded on a Cary 5000 spectrometer from Varian Inc. The fluorescence spectra were measured with a Spectronics Instruments 8100 spectrofluorometer 8100 recently described.<sup>65</sup> Standard quartz cuvettes (Hellma) with an optical path length of 1 cm were used. The fluorescence decays were measured using the time-correlated single-photon counting technique with a FluoTime200 spectrofluorimeter equipped with a TimeHarp200 TCSPC board (PicoQuant).<sup>66</sup> A diode laser (LDH470 driven by PDL800-B driver, PicoQuant) emitting at 466 nm (fwhm 6 nm, optical pulse duration 72 ps) was used for excitation. Because of the long lifetime of QDs, the pulse repetition rate was reduced to 2.5 or 5 MHz, corresponding to 400 or 200 ns pulse spacing. The overall instrument response function fwhm was 330 ps. The detection wavelength was 578 nm (spectral bandwidth 4 nm) for the CdSe–DCM experiment and 576 nm (spectral bandwidth 8 nm) for the InP–CdSe experiment. To assess the reproducibility of the decomposition approach, four independent measurements were performed and the standard deviation for each mixing ratio was calculated. The decomposition of the decay curves and the fitting of the fluorescence lifetimes was done using the SymPho-

Time software package from PicoQuant.<sup>67</sup> All the fluorescence measurements were performed in a 90° excitation–emission (L-) geometry using magic angle conditions with the excitation polarizer set to 0° (vertical polarization) and the emission polarizer set to 54.7° in order to eliminate possible polarization effects.

**Materials.** Toluene was used for all the measurements and was of spectroscopic grade and purchased from Sigma-Aldrich. Prior to use, it was checked for fluorescent impurities. The InP/ZnS and CdSe/ZnS core/shell quantum dots were synthesized as described in refs 68 and 69, respectively. DCM (4-(dicyanomethylene)-2-methyl-6-(*p*-dimethylaminostyryl)-4*H*-pyran) was purchased from Lambda Physics. The approximate chromophore concentration of the solutions of the pure components were calculated from the measured absorbances using the molar absorption coefficients reported by refs 70 and 71 for CdSe and InP, respectively, and on the basis of the molar absorption coefficients given in ref 72 for DCM.

**Safety Considerations.** Proper safety procedures for the handling, storage, and disposal of CdSe QDs should be observed.

## RESULTS AND DISCUSSION

QDs show fluorescence lifetimes in the order of 10–100 ns with typically multiexponential decay kinetics<sup>73,74</sup> in addition to their extremely broad absorption and narrow emission spectra,

- (63) Fisher, B. R.; Eisler, H. J.; Stott, N. E.; Bawendi, M. G. *J. Phys. Chem. B* **2004**, *108*, 143–148.
- (64) Schlegel, G.; Bohnenberger, J.; Potapova, I.; Mews, A. *Phys. Rev. Lett.* **2002**, *88*, 137401.
- (65) Resch-Genger, U.; Pfeifer, D.; Monte, C.; Pilz, W.; Hoffmann, A.; Spieles, M.; Rurack, K.; Hollandt, J.; Taubert, D.; Schonenberger, B.; Nording, P. *J. Fluoresc.* **2005**, *15*, 315–336.
- (66) Bohmer, M.; Pampaloni, F.; Wahl, M.; Rahn, H.-J.; Erdmann, R.; Enderlein, J. *Rev. Sci. Instrum.* **2001**, *72*, 4145–4152.
- (67) [http://www.picoquant.com/products/sw\\_mt/sw\\_mt.htm](http://www.picoquant.com/products/sw_mt/sw_mt.htm).
- (68) Xu, S.; Ziegler, J.; Nann, T. *J. Mater. Chem.* **2008**, *18*, 2653–2656.
- (69) Ziegler, J.; Merkulov, A.; Grabolle, M.; Resch-Genger, U.; Nann, T. *Langmuir* **2007**, *23*, 7751–7759.
- (70) Yu, W. W.; Qu, L.; Guo, W.; Peng, X. *Chem. Mater.* **2003**, *15*, 2854–2860.
- (71) Adam, S.; Talapin, D. V.; Borchert, H.; Lobo, A.; McGinley, C.; de Castro, A. R. B.; Haase, M.; Weller, H.; Moller, T. *J. Chem. Phys.* **2005**, *123*, 084706–084710.
- (72) Du, H.; Fuh, R. A.; Li, J.; Corkan, A.; Lindsey, J. S. *Photochem. Photobiol.* **1998**, *68*, 141–142.
- (73) Labeau, O.; Tamarat, P.; Lounis, B. *Phys. Rev. Lett.* **2003**, *90*, 257404–257401; 257404–257404.



favorable for color multiplexing (see Figure 1). For most QDs, at least three decay terms are necessary to describe the fluorescence decay kinetics satisfactorily (see Figure 6). In the most simple case of combining a QD with an organic dye with a monoexponential fluorescence decay, this already results in four decay terms. This represents the limit of a reasonable simulation for nonlinear least-squares curve fitting, which is generally used to analyze such multiexponential decays.<sup>75</sup> Experiments with three luminescent species or the combination of two QDs renders this situation even more complex. Thus, the value of QDs for lifetime multiplexing is clearly limited when using this conventional approach.

**Data Analysis.** We have chosen a different approach to overcome these limitations: instead of analyzing the decays in terms of exponential functions, we pursued a simple type of “pattern-matching”, yet in the time domain. (A similar procedure to identify fluorophores by their decay pattern is reported in ref 76.) In our method of analysis, the decay curve is described as a linear combination of the decay curves of the individual components present in the mixture. With the use of time-correlated single-photon counting, the fluorescence intensity at a given time after the excitation light pulse is represented as the number of photons  $N(i)$  in the corresponding time channel  $i$ . For a system containing two components, A and B, the fluorescence decay can then be described by eq 1.

$$N_M(i) = aN_A(i) + bN_B(i) \quad (1)$$

Here,  $N_M(i)$  is the number of photons of the mixture in the time channel  $i$  and  $N_A(i)$  and  $N_B(i)$  are the corresponding photon numbers recorded for the fluorescence decays of the pure components. The factors  $a$  and  $b$  are the contributions of components A and B to the decay of the mixture M. If each curve is normalized to the total photon number of the decay according to eq 2,

$$N(i) = \frac{N_{\text{raw}}(i)}{\sum_i N_{\text{raw}}(i)} \quad (2)$$

and the concentration of the pure components are adjusted to yield the same fluorescence intensity, the factors  $a$  and  $b$  directly yield the intensity fraction of the respective component to the total fluorescence intensity of the mixture. In the case of unequal fluorescence intensities, these differences can be corrected by dividing  $a$  and  $b$  by the respective intensity values. The factors  $a$  and  $b$  are obtained by fitting  $N_M(i)$  to the measured decay of the mixture,  $N_{\text{exp}}(i)$ . According to photon statistics (Poisson statistics), this is done by minimization of  $\chi^2$  according to eq 3 (see, e.g., ref 75).

$$\chi^2 = \sum_i \frac{(N_M(i) - N_{\text{exp}}(i))^2}{N_{\text{exp}}(i)} \quad (3)$$

(74) van Sark, W. G. J. H. M.; Frederix, P. L. T. M.; van den Heuvel, D. J.; Bol, A. A.; van Ling, J. N. J.; de Mello Donega, C.; Gerritsen, H. C.; Meijerink, A. *J. Fluoresc.* **2002**, *12*, 69–76.

(75) Birch, D. J. S.; Imhof, R. E. In *Topics in Fluorescence Spectroscopy: Techniques*; Lakowicz, J. R., Ed.; Plenum Press: New York, 1991; Vol. 1, pp 1–95.

(76) Enderlein, J.; Sauer, M. *J. Phys. Chem. A* **2001**, *105*, 48–53.

**Table 1. Mixing Ratios of CdSe and DCM, Corresponding Volume Fractions of CdSe in the Mixtures, the Simulation (Decomposition) Results, the Relative Differences from the Theoretical Values, and the Relative Standard Deviations for the Decomposition Results**

| mixing ratio CdSe/DCM | fraction of CdSe | decomposition result CdSe | relative difference (%)   | relative standard deviation (%) |
|-----------------------|------------------|---------------------------|---------------------------|---------------------------------|
| 1:31                  | 0.03125          | 0.0290                    | −7.1                      | 6.4                             |
| 1:15                  | 0.0625           | 0.0639                    | 2.2                       | 4.3                             |
| 1:7                   | 0.125            | 0.1321                    | 5.7                       | 3.2                             |
| 1:3                   | 0.25             | 0.2482                    | −0.7                      | 2.0                             |
| 1:1                   | 0.5              | 0.5024                    | 0.5                       | 1.4                             |
| 3:1                   | 0.75             | 0.7544                    | 0.6 (−1.7 <sup>a</sup> )  | 0.8 (2.5 <sup>a</sup> )         |
| 7:1                   | 0.875            | 0.8646                    | −1.2 (8.3 <sup>a</sup> )  | 0.8 (5.4 <sup>a</sup> )         |
| 15:1                  | 0.9375           | 0.9372                    | −0.03 (0.5 <sup>a</sup> ) | 0.7 (10 <sup>a</sup> )          |
| 31:1                  | 0.96875          | 0.9680                    | −0.08 (2.4 <sup>a</sup> ) | 0.4 (13 <sup>a</sup> )          |

<sup>a</sup> Corresponding values for the fraction of DCM.

**Table 2. Mixing Ratios of InP and CdSe, Corresponding Volume Fractions of InP in the Mixtures, the Simulation (Decomposition) Results and the Relative Differences from the Theoretical Values, and the Relative Standard Deviations for the Decomposition Results**

| mixing ratio InP/CdSe | fraction of InP | decomposition result InP | relative difference (%)  | relative standard deviation (%) |
|-----------------------|-----------------|--------------------------|--------------------------|---------------------------------|
| 1:9                   | 0.10            | 0.100                    | 0                        | 9.2                             |
| 1:3                   | 0.25            | 0.211                    | −15                      | 9.6                             |
| 1:1                   | 0.50            | 0.485                    | −3.1                     | 5.7                             |
| 3:1                   | 0.75            | 0.721                    | −3.8 (11 <sup>a</sup> )  | 3.2 (8.2 <sup>a</sup> )         |
| 9:1                   | 0.90            | 0.908                    | 0.9 (−7.9 <sup>a</sup> ) | 2.1 (20 <sup>a</sup> )          |

<sup>a</sup> Corresponding values for the fraction of CdSe.

This decomposition procedure is independent of the actual shape of the decay curve. Accordingly, not only multiexponential decays can be properly analyzed with this approach, also nonexponential decays or any other complex decay kinetics. The sole prerequisite is that the shapes of the decay curves of the individual components differ sufficiently to enable a clear distinction between them. Furthermore, this method is independent of the individual characteristics of the measurement equipment (artifacts). In particular, no deconvolution of the measured decays with the instrument response function is necessary, which is normally mandatory for the accurate analysis of at least short fluorescence lifetimes obtained with time-correlated single-photon counting measurements.<sup>77</sup>

In addition to the prerequisite of sufficiently different fluorescence decay kinetics, the pairs of chromophores used in the binary mixtures were chosen to show absorption in the same wavelength region and to emit at the same wavelength in order to allow for efficient simultaneous excitation at a single wavelength, here 466 nm, and to enable fluorescence detection at a single detection wavelength. The mixtures of a QD and an organic dye (see section CdSe–DCM) and two different QDs (see section InP–CdSe) were prepared by simply mixing different volumes of the toluene solutions of the pure components (see Tables 1 and 2). The concentration of the pure components were adjusted to yield equal

(77) van de Ven, M.; Ameloot, M.; Valeur, B.; Boens, N. *J. Fluoresc.* **2005**, *15*, 377–413.

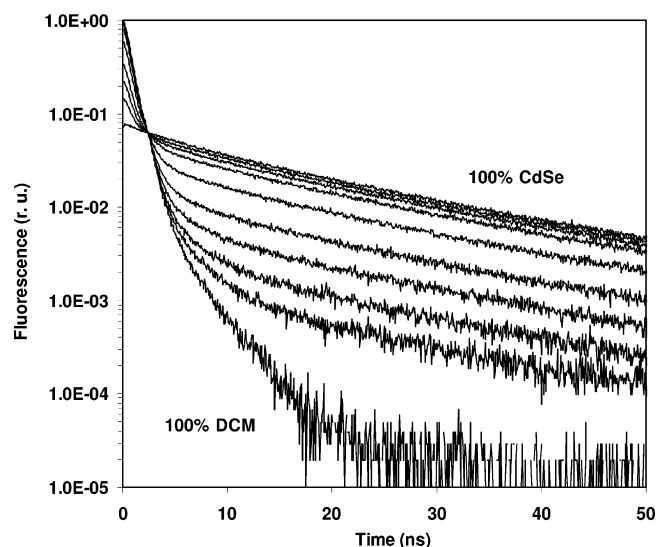


**Figure 2.** Fluorescence decays of pure CdSe and DCM and the different mixtures of both components (excitation 466 nm; detection 578 nm). The decays are normalized to equal areas under the decay curves. Fluorescence was measured up to 200 ns after the excitation pulse. For better illustration, only the first 50 ns are shown.

fluorescence intensities at the detection wavelength when excited at 466 nm in order to keep the analysis as simple and straightforward as possible. The decay curves of the pure components and the mixtures, varying in the relative ratios of the two components, were recorded using identical measurement conditions and the analysis of the decays was performed as described in the previous section. To account for a possible dependence of the fluorescence lifetimes on chromophore concentration that may result for QDs due to ligand adsorption–desorption equilibria,<sup>78,79</sup> the decays of the pure components were also measured at concentrations that correspond to the highest dilution (lowest concentration) used in the mixtures. No concentration-dependent change in decay behavior was found for all of the samples analyzed.

**CdSe–DCM.** CdSe with a passivating ZnS-shell (CdSe/ZnS) was used as a representative QD label in conjunction with the organic dye DCM. The excitation wavelength was 466 nm (fwhm 6 nm), and the detection wavelength was set to the maximum of the CdSe emission at 578 nm (spectral bandpass 4 nm), as indicated by the arrows in Figure 1. The concentration of the solutions was approximately  $4.8 \times 10^{-6}$  M for DCM and  $1.3 \times 10^{-7}$  M for CdSe. The CdSe particles showed the expected multiexponential fluorescence decay, see Figure 2. Four decay times, i.e., 4.2, 15, 32, and 131 ns with relative amplitudes of 0.23, 0.62, 0.14, and 0.01, respectively, were necessary to describe the measured decay curve adequately. The average fluorescence lifetime, calculated according to ref 80, was 28 ns ( $\tau_{1/e}$  was 13 ns). DCM is known to show a double exponential fluorescence decay. We found lifetimes of 0.74 and 2.6 ns in toluene with relative amplitudes of 0.98 and 0.02, respectively. The resulting average fluorescence lifetime was 0.85 ns ( $\tau_{1/e}$  was 0.90 ns). These values are in the range of the values given for DCM in

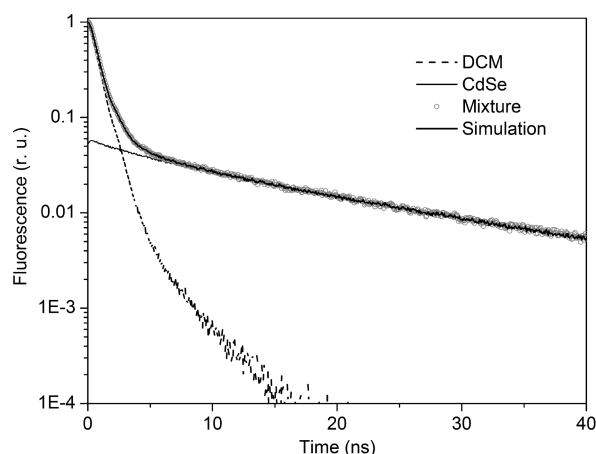


**Figure 3.** Illustration of the decomposition principle for a 1:1 mixture of CdSe and DCM. The decay of the mixture (○) is fitted by the sum (thick line) of the decays of CdSe (thin line) and DCM (dashed line).

polar solvents like methanol and acetonitrile and in chloroform (0.20–0.57 and 1.37–1.97 ns<sup>81</sup>) but significantly longer than the value reported for toluene (0.20 and 0.65 ns<sup>82</sup>).

The resulting decay curves for the various mixtures of CdSe and DCM, together with the decays of the pure components, are shown in Figure 2. All the decays are normalized to equal areas below the decay curves and show a clear isosbestic point as to be expected for such a binary mixture. The decomposition approach used by us, see previous section, is illustrated in Figure 3 for a 1:1 mixture showing the measured decays of both pure components and the sum of these decay curves together with the decay of the mixture. This leads to a time-integrated intensity of the mixed decay twice as high as in the real measurement, see Figure 2. The ratios used for CdSe and DCM and the corresponding volume fractions of CdSe are given in Table 1, together with the results of the lifetime analysis that is also summarized in Figure 4. We find a very good agreement between the CdSe fractions obtained by the decomposition procedure and the volume fractions in the mixtures. In the data analysis, a correction was applied in order to account for the relatively high absorbance of the pure DCM component at the excitation wavelength as compared to the absorbance of the CdSe (0.20 for DCM, 0.033 for CdSe) which would otherwise result in a systematic error caused by the inner filter effect of the excitation light. For the mixing ratio of 1:15 (CdSe fraction of 0.0625), the relative error (standard deviation), derived from 8 independent measurements, was determined to 4%.

**InP–CdSe.** In addition, the potential of a mixture of two QDs as a set of multiplex chromophores was investigated. Here, we have chosen InP passivated with a ZnS-shell (InP–ZnS) and ZnS-shelled CdSe. The absorption and emission spectra of both QDs are shown in Figure 5. The concentration of the pure components was approximately  $2.7 \times 10^{-7}$  M for InP and  $2 \times 10^{-8}$  M for CdSe, respectively. The absorbance at the excitation wavelength of 466 nm (spectral width 6 nm) was 0.035 and 0.0043, respectively. As in the previous experiment, the detection wavelength was set to the maximum of the CdSe emission at 576 nm

(78) Ji, X. H.; Copenhaver, D.; Sichmeller, C.; Peng, X. G. *J. Am. Chem. Soc.* **2008**, *130*, 5726–5735.

(79) Munro, A. M.; Plante, I. J. L.; Ng, M. S.; Ginger, D. S. *J. Phys. Chem. C* **2007**, *111*, 6220–6227.

(80) Lakowicz, J. R. *Principles of Fluorescence Spectroscopy*, 3rd ed.; Kluwer Academic: New York, 2006.

(81) Meyer, M.; Mialocq, J. C. *Chem. Phys. Lett.* **1988**, *160*, 484–490.

(82) Turban, A. A.; Bondarev, S. L.; Knyukshto, V. N.; Stupak, A. P. *J. Appl. Spectrosc.* **2006**, *73*, 678–685.

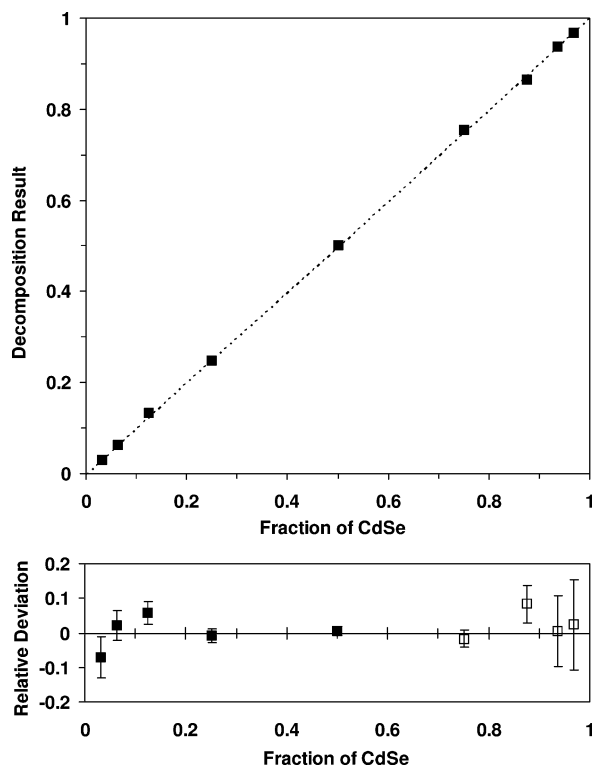


**Figure 4.** Decomposition result obtained for the mixtures of the CdSe–DCM studies. Shown are the fractions of CdSe in the mixtures that result from the decomposition in dependence of the volume fractions used in the mixture (upper panel). For a perfect decomposition, the points should be located at the dotted line. The relative differences from the expected values and the relative standard deviations are displayed in the lower panel (■). For a better visualization of the deviations, at CdSe fractions above 0.5 the corresponding values for the DCM decomposition results are displayed (□ in lower panel).

(spectral bandpass 8 nm) as indicated by the arrows in Figure 5. The InP QDs showed a significantly slower, yet similar, multiexponential fluorescence decay as compared with the CdSe particles. Also for InP, four decay times were required to describe the fluorescence decay (2.5, 14, 49, and 167 ns, relative amplitudes 0.27, 0.31, 0.35, and 0.06). The average fluorescence lifetime of InP was determined to 82 ns and  $\tau_{1/e}$  was 17 ns. A four-

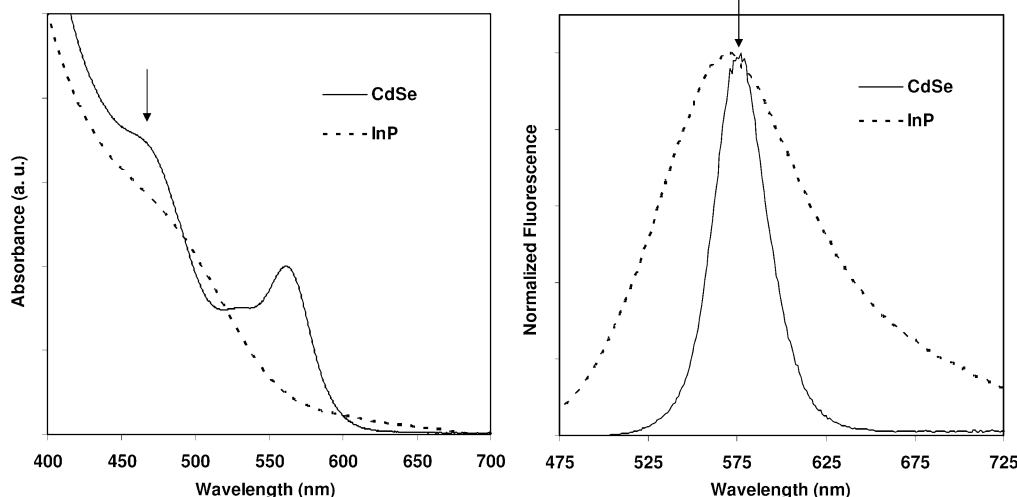


**Figure 5.** Absorption (left) and fluorescence (right) spectra of InP quantum dots (solid lines) and CdSe quantum dots (dashed lines) used for the InP–CdSe studies. The arrows indicate the chosen excitation (466 nm) and detection (576 nm) wavelength.

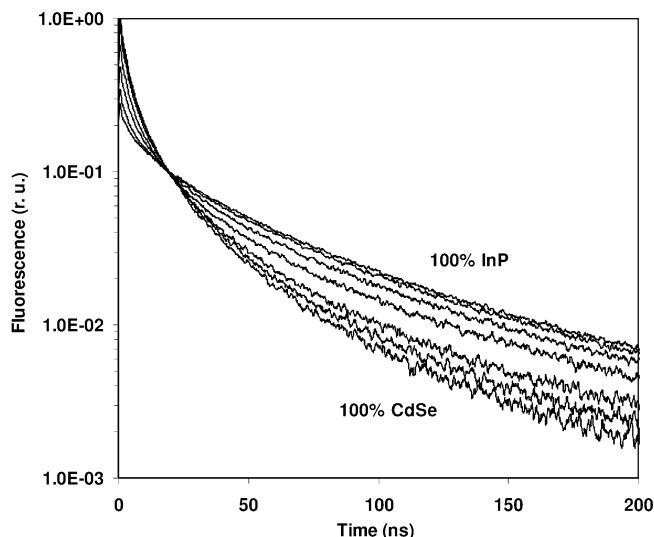


**Figure 6.** Fluorescence decays of InP, CdSe, and the different mixtures of both components (excitation 466 nm; detection 576 nm). The decays are normalized to equal areas under the curves. Fluorescence was measured up to 400 ns after the excitation pulse; for a better illustration, only the first 200 ns are shown.

exponential fit for the CdSe-sample used in this experiment resulted in decay times of 2.4, 9.2, 31, and 130 ns with relative amplitudes of 0.57, 0.33, 0.09, and 0.01. The corresponding average fluorescence lifetime was 29 ns and  $\tau_{1/e}$  was 4.3 ns.

Figure 6 shows the area-normalized decay curves of the mixtures and the pure components. As observed for the CdSe–DCM mixtures, the decay curves of the CdSe–InP mixtures also display an isosbestic point. The mixing ratios of both components, the corresponding volume fractions of InP, and the decomposition results highlighted in Figure 7 are summarized in Table 2. Also for this mixture of two QDs, we find good agreement of the fitting results and the expected values as determined from the mixing ratios. The deviations are slightly larger than those observed in the CdSe–DCM experiment. This is most likely due to the fact that the decay kinetics of InP and CdSe exhibit smaller differences as in the case of the CdSe–DCM pair. The decomposition results for the InP fraction seems to be systematically

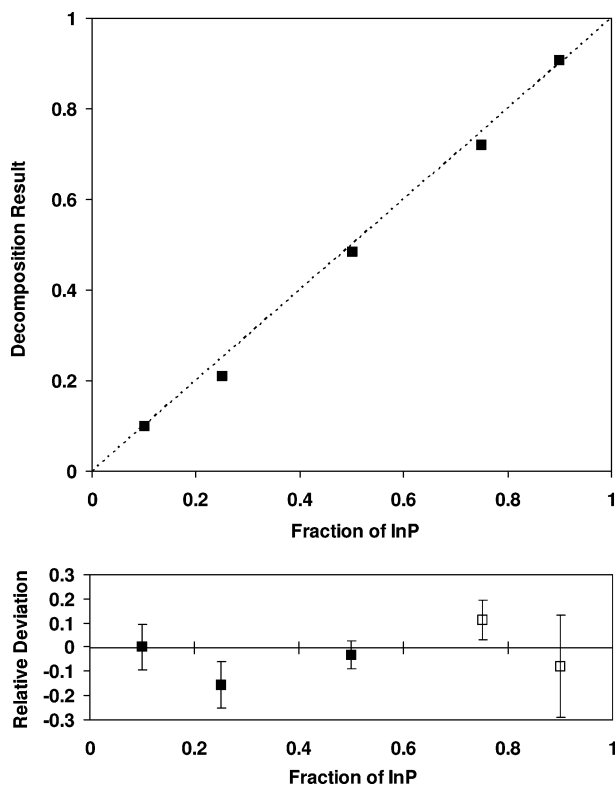


**Figure 7.** Decomposition data resulting for the InP–CdSe mixtures. Shown are the fractions of InP in the mixtures that result from the decomposition in dependence of the volume fractions used in the mixture (upper panel). For a perfect decomposition, the points should be located at the dotted line. The relative differences from the expected values and the relative standard deviations are displayed in the lower panel (■). For a better visualization of the deviations at InP fractions above 0.5, the corresponding values for the CdSe decomposition results are displayed (□ in lower panel).

smaller than the theoretical values. This could in principle be attributed to FRET between both QDs, according to overlap of their absorption and emission spectra (see Figure 5), predominately from InP to CdSe. Such an energy transfer from excited InP to CdSe should result in a partial depopulation of the excited state of InP and a concomitant increase of excited CdSe particles, leading to a faster overall fluorescence decay of the mixture and thus to an underestimation of the slow decaying InP component. However, for CdSe, a mean distance between nearest neighbors of about 400 nm can be estimated for the highest particle concentration used in the mixtures. This is far beyond the limit

of about 10 nm for efficient FRET.<sup>83–85</sup> Only if the particles agglomerate, energy transfer should be possible thereby accounting for the observed small deviations. In the case of the CdSe–DCM mixture, no hint for FRET, here from DCM to CdSe (cf. Figure 1) leading to an overestimation of the CdSe fraction was observed, despite the higher CdSe concentration used.

## CONCLUSIONS AND OUTLOOK

A simple decomposition procedure was developed that enables the lifetime analysis of any complex decay kinetics independent of the individual characteristics of the measurement equipment, provided that the shapes of the decay curves of the individual components differ sufficiently. Pursuing this simple type of “pattern-matching” in the time domain, we were for the first time able to accurately decompose mixtures of a QD and an organic dye and mixtures of two QDs. This demonstrates the principal suitability of multiexponentially decaying QDs as multiplex chromophores. The proper choice of the spectral characteristics of these chromophores are crucial to circumvent FRET-induced changes in fluorescence lifetime that may otherwise lead to small distortions of the quantification of the decaying species.

In the future, we will investigate the potential of this approach for multicolor lifetime multiplexing with mixtures of QDs with spectrally matching short-lived organic dyes and QDs. Advantageous for multicolor lifetime multiplexing with QDs can be the fact that FRET between QDs of varying size and/or constituent material, and thus in the spectral position of their absorption and emission bands, is typically less efficient as FRET between organic dyes due to the ligand shell that introduces a certain spatial separation of such QDs. Accordingly, different types of ligands and shells varying in thickness will be investigated with respect to their potential to control and minimize FRET.

## ACKNOWLEDGMENT

Financial support from the German Ministry of Education and Research (BMBF; Grant 13N8849) is gratefully acknowledged.

Received for review May 1, 2009. Accepted August 4, 2009.

AC900934A

(83) Förster, T. *Ann. Phys.* **1948**, 437, 55–75.

(84) Sapsford, K. E.; Berti, L.; Medintz, I. L. *Angew. Chem., Int. Ed.* **2006**, 45, 4562–4588.

(85) Stryer, L. *Annu. Rev. Biochem.* **1978**, 47, 819–846.